

Organic & Biomolecular Chemistry

Accepted Manuscript



This is an *Accepted Manuscript*, which has been through the Royal Society of Chemistry peer review process and has been accepted for publication.

Accepted Manuscripts are published online shortly after acceptance, before technical editing, formatting and proof reading. Using this free service, authors can make their results available to the community, in citable form, before we publish the edited article. We will replace this *Accepted Manuscript* with the edited and formatted *Advance Article* as soon as it is available.

You can find more information about *Accepted Manuscripts* in the [Information for Authors](#).

Please note that technical editing may introduce minor changes to the text and/or graphics, which may alter content. The journal's standard [Terms & Conditions](#) and the [Ethical guidelines](#) still apply. In no event shall the Royal Society of Chemistry be held responsible for any errors or omissions in this *Accepted Manuscript* or any consequences arising from the use of any information it contains.

ARTICLE

Synthesis, Characterization and Biological Evaluation of Carboranyl methylbenzo[*b*]acridones as Novel Agents for Boron Neutron Capture Therapy

Cite this: *Org. Biomol. Chem.*, 2014,
DOI: 10.1039/x0xx00000x

DOI: 10.1039/x0xx00000x

www.rsc.org/

A. Filipa F. da Silva,^a Raquel S. G. R. Seixas,^a Artur M. S. Silva,^a Joana Coimbra,^{a§} Ana C. Fernandes,^b Joana P. Santos,^{‡b} António Matos,^c José Rino,^d Isabel Santos^b and Fernanda Marques^{*b}

Herein we present the synthesis and characterization of benzo[*b*]acridin-12(*7H*)-ones bearing carboranyl moieties and test their biological effectiveness as boron neutron capture therapy (BNCT) agents in cancer treatment. The cellular uptake of these novel compounds into the U87 human glioblastoma cells was evaluated by boron analysis (ICP-MS) and by fluorescence imaging (confocal microscopy). The compounds enter the U87 cells exhibiting a similar profile *i.e.*, preferential accumulation in the cytoskeleton and membranes and low cytotoxic activity (IC₅₀ values higher than 200 μM). The cytotoxic activity and cellular morphological alterations after neutron irradiation in the Portuguese Research Reactor (6.6 × 10⁷ neutrons cm⁻² s⁻¹, 1 MW) were evaluated by the MTT assay and by electronic microscopy (TEM). Post-neutron irradiation revealed that BNCT has a higher cytotoxic effect on the cells. Accumulation of membranous whorls in the cytoplasm of cells treated with one of the compounds correlates well with the cytotoxic effect induced by radiation. Results provide a strong rationale for considering one of these compounds as a lead candidate for a new generation of BNCT agents.

Keywords: DNA intercalators; fluorescent probes; Benzo[*b*]acridones; dodecarboranes; Boron Neutron Capture Therapy

Introduction

Malignant gliomas are the most common type of primary malignant brain tumour and most frequently found brain tumour diagnosed in up to 49% of cases. According to the World Health Organization (WHO) glioblastoma or grade IV glioma is the most common form of gliomas and represent one of the most aggressive and treatment resistant type of

human cancer.^{1,2} Glioblastoma remain an incurable disease despite technological and therapeutic improvements in surgery, radiotherapy and chemotherapy or combined therapeutic modalities. The outlook has improved only modestly, and the survival rate of patients stays less than a few percent.^{3,4} The therapeutic challenge is to develop strategies that can selectively target malignant cells, with little

or no effect on normal cells and tissues adjacent to the tumour. One such approach is the so called “binary therapy” in which two non-toxic components can be combined in order to produce a cytotoxic effect.^{5,6} The advantage is that each component can be modulated and manipulated independently to maximize the therapeutic efficacy.

A potential useful binary system is the boron neutron capture therapy (BNCT). As a binary treatment modality, BNCT combines a radiosensitizer, ^{10}B (19.8% natural abundance) with thermal neutrons (n), an indirectly ionizing radiation. The subsequent (n,α) reaction yields 1.47 MeV α particles and 0.84 MeV ^7Li ions, both having high linear energy transfer (LET) causing radiotoxic effects in the range of a cell diameter (*ca.* 10 μm). The efficient energy transfer produces selective damage in the cells containing ^{10}B so that boron content and distribution in tumour are pivotal to the therapeutic efficacy of this treatment modality.⁵⁻⁷

Boron atoms have to be targeted to tumour cells using a suitable boron carrier in order to maximize tumour cell damage and minimize total radiation dose to the patient. The boron drugs sodium borocaptate (BSH) and boronophenylalanine (BPA) have been extensively studied and are currently approved to treat glioma, melanoma, head and neck tumours and hepatocarcinoma.⁸⁻¹⁰ These compounds are however far from ideal, exhibiting insufficient selectivity and efficiency, besides other limitations such as reduced capability to cross the blood brain barrier (BBB) and poor water solubility (BPA).¹¹⁻¹³ The subcellular distribution of these compounds in a glioma cell model showed that most of

the boron was localized in the cytoplasm of the cells, but only minimal concentrations of boron in the nuclei.¹⁴

The major challenge in the development of boron delivery agents is to deliver a sufficient amount of boron into the tumour cells to maximize the doses of radiation to the tumour with minimal normal tissue toxicity.¹⁵ The use of boron clusters such as a dodecarborane instead of single boron atoms, allows increasing loading ability. Moreover, dodecarborane contain 10 boron atoms and possess a rather low cytotoxicity and is compatible and extremely stable in biological media.^{16,17} To increase the selectivity and efficacy of dodecarboranes towards cancer cells a large variety of derivatives have been designed and evaluated, taking into account specific features of cancer cells, such as enhanced metabolism and over-expression of target receptors.¹⁸⁻²² DNA binding agents and tumour seeking molecules like porphyrins and porphyrinic macrocyclic compounds, such as phthalocyanines, are also alternatives for selective delivery of boron moiety into tumour cells.²³⁻²⁷ However, until now there is no new boron compound that has reached the stage for phase I clinical trials. Both BSH and BPA still remain today as the only two drugs in clinical trial for BNCT.²⁸

Research in BNCT involves the design, synthesis and evaluation of more selective tumour targeting agents. The close proximity of the boron agent to DNA of tumour cells is also highly desirable. DNA intercalators such as acridine and acridone derivatives are excellent candidates since they target the DNA and, at the same time, act as fluorescent probes to follow them inside the cells.²⁹⁻³³ In addition, these compounds

have attracted considerable attention from scientific community due to their wide range of biological activities.³⁴⁻

³⁶ Benzo[*b*]acridones are much less studied than acridones.

The most common derivatives of this type of compounds are benzo[*b*]acronycines which present potent broad spectra of antitumour activities.^{37,38} The application of these compounds as fluorescent probes was also described.³⁹

Due to our interest in the search for novel antitumour agents, here we present the synthesis, and preliminary biological evaluation of a series of acridone and benzo[*b*]acridone derivatives bearing carboranyl moieties and the evaluation of its potential as BNCT agents. These results may offer new insights for consideration in malignant glioma treatment strategies.

Results and discussion

Synthesis

The main goal of this study was to prepare benzo[*b*]acridin-12(*7H*)-ones bearing carboranyl methyl moieties attached to the nitrogen atom as suitable agents for BNCT. Benzo[*b*]acridin-12(*7H*)-ones **1a-c** were synthesized through a two-steps method developed by our group.⁴⁰

Propargylation of benzo[*b*]acridin-12(*7H*)-ones **1a-c** was first attempted by refluxing benzo[*b*]acridin-12(*7H*)-one (**1a**) with an excess of propargyl bromide in acetone using potassium carbonate as base, although even after a long reaction time (20 h) there was still remaining 39% of starting material. Beside this, two new compounds were isolated, one corresponding to the expected propargylated benzo[*b*]acridin-

12(*7H*)-one **2a** (30%) and the other to 7-(propa-1,2-dien-1-yl)benzo[*b*]acridin-12(*7H*)-one **3** (15%) (Fig. 1).

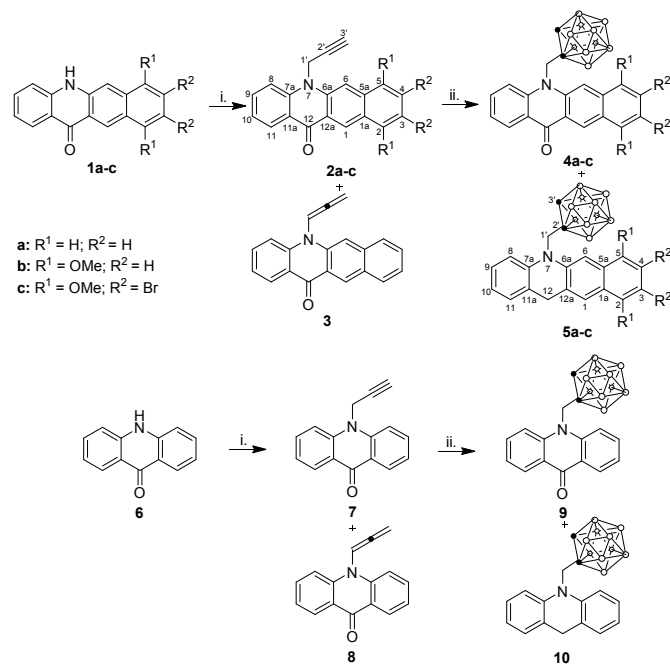


Fig. 1 Synthetic pathway for the preparation of 7-carboranylmethylbenzo[*b*]acridin-12(*7H*)-ones **4a-c** and 10-carboranylmethylacridin-9(*10H*)-one (**9**). Reagents and conditions: i. BrH₂CC≡CH, NaH, THF (dry), 40 °C, N₂; ii. B₁₀H₁₄, CH₃CN, toluene, 80 °C, N₂. ● = C or C-H; ○ = B-H.

Since the obtained yields were not satisfactory and the reaction time was too long it was decided to replace potassium carbonate for sodium hydride (2 equiv) and the reaction was carried out in dry THF. After refluxing the reaction mixture for 4 h it was observed the complete disappearance of benzo[*b*]acridin-12(*7H*)-one (**1a**) and the formation of the desired 7-(prop-2-yn-1-yl)benzo[*b*]acridin-12(*7H*)-one (**2a**) in good yield (72%), being the corresponding allene **3** isolated in 22% yield. After several attempts using different amounts of base and temperatures, the optimal conditions were found and considered the use of

1.8 equiv of sodium hydride in dry THF at 40 °C during 2 h and allowed to obtain only the propargylated benzo[*b*]acridin-12(7*H*)-one **2a** in good yield (86%). It was observed that the formation of the allene **3** is promoted by increasing the amount of sodium hydride. The reaction of **1b,c** with propargyl bromide under the conditions described above gave the corresponding propargylated derivatives **2b,c** in good yields (75% and 76%, respectively). These conditions were also used for the propargylation of the commercial acridin-9(10*H*)-one (**6**) and allowed the synthesis of 10-(prop-2-yn-1-yl)acridin-9(10*H*)-one (**7**) in very good yield (92%) although, as observed for the case of benzo[*b*]acridin-12(7*H*)-one (**1a**), the use of 2 equiv of sodium hydride promoted the formation of 10-(propa-1,2-dien-1-yl)acridin-9(10*H*)-one (**8**).

The cycloaddition reaction of the propargyl triple bond with decaborane were performed following a linear procedure based on the reaction of acetylenic moiety with a bis(acetonitrile)decaborane complex.⁴¹ There are some methodologies concerning this type of reaction. Some authors described that bis(acetonitrile)decaborane complex must be formed, by reacting decaborane with acetonitrile in toluene for 1 h, before the reaction with the acetylenic compound.⁴² In the first attempt to prepare carboranylmethylbenzo[*b*]acridin-12(7*H*)-one (**4a**), **2a** was left reacted with 1.5 equiv of decaborane at 80 °C for 24 h, then a new main product was isolated and after characterization revealed to be the corresponding cycloadduct bearing the acridone carbonyl group hydrogenated **5a** (45%). Similar results were obtained in the reaction of 7-(prop-2-yn-1-yl)benzo[*b*]acridin-12(7*H*)-

ones **2b,c** with decaborane (for **2b** the reaction proceed in 30 h and afforded 37% of the dihydroacridine **5b** and for **2c** the reaction proceed in 24 h and afforded 30% of the dihydroacridine **5c**).

Trying to understand the reaction mechanism it was decided to perform some studies with commercial available acridin-9(10*H*)-one (**6**), since the synthetic pathway of benzo[*b*]acridones involves many steps. Cycloaddition reaction of 10-(prop-2-yn-1-yl)acridin-9(10*H*)-one (**7**) with decaborane afforded after 20 h, under the reaction conditions described above, the 10-carboranylmethyl-9,10-dihydroacridine (**10**) in moderate yield (30%). This result led us to reduce the reaction time trying to get the desired adduct **9**; after 1 h the reaction was stopped since product **10** began to be observe. After reaction mixture purification, dihydroacridine **10** was isolated in 15% yield and a second product with a similar R_f value to acridin-9(10*H*)-one **7**, that after characterization was identified as the 10-carboranylmethylacridin-9(10*H*)-one (**9**) (63%) (Fig. 1). Thus, it was proved that 10-carboranylmethylacridin-9(10*H*)-one (**9**) is formed in the reaction and over time is completely reduced to the corresponding dihydro derivative **10**.

Therefore, the cycloaddition reaction of 7-(prop-2-yn-1-yl)benzo[*b*]acridin-12(7*H*)-ones **2a-c** with decaborane were performed and finished when the appearance of the dihydroacridine derivative **5a-c** was saw, since the R_f value of 7-carboranylmethylbenzo[*b*]acridin-12(7*H*)-ones **4a-c** were very similar to the corresponding starting materials **2a-c**. After 2 h for derivatives **2a** and **2b** and 4 h for derivative **2c**

7-carboranylmethylbenzo[*b*]acridin-12(7*H*)-ones **4a-c** (**4a**: 53%; **4b**: 46%; **4c**: 45%) were obtained as major products, although the corresponding 7-carboranylmethyl-7,12-dihydrobenzo[*b*]acridines **5a-c** (**5a**: 22%; **5b**: 15%; **5c**: 19%) were always isolated as by-products.

Cytotoxicity

In order to evaluate the cytotoxicity of compounds and also to select a dose for irradiation, the U87 human glioma cells, a clinically relevant tumour cell line for BNCT, were treated with compounds **9**, **4a-4c** in the concentration range 5-200 μM for 6 h continuous incubation at 37°C. A low cytotoxicity for a boronated agent is an important parameter in BNCT so that boron concentrations within tumours can be maximised. The cytotoxic activity of the boron compounds was determined using the MTT assay which evaluates the reduction of the tetrazolium salt by a mitochondrial dehydrogenase in metabolic active cells to insoluble formazan crystals.⁴³ The cellular viability in the presence of the tested compounds was compared to that observed in controls (no additions) and the cellular viability (%) was calculated. The corresponding inhibition curves (effect on cellular viability vs. compound concentration) are depicted in Fig. 2. As can be observed the boron compounds **4a-4c** did not show activity against the U87 cells in the range 5-200 μM . However, compound **9**, the 7-carboranylmethylacridin-9(10*H*)-one seemed to be more active presenting an IC_{50} value of $225.0 \pm 61.3 \mu\text{M}$.

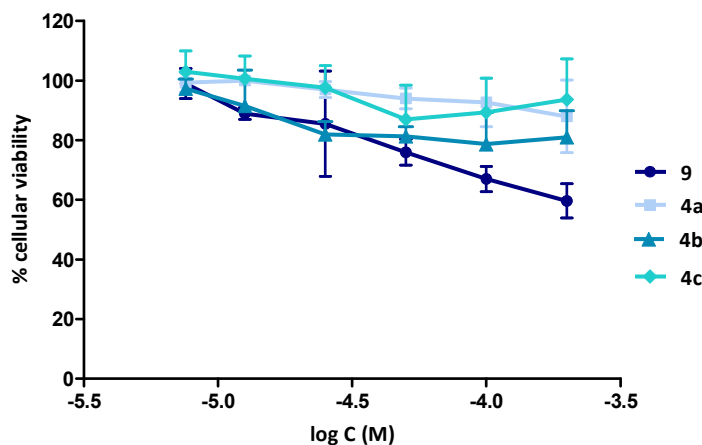


Fig. 2 Cellular viability (%) of U87 cells after a 6 h treatment period with the boron compounds **9**, **4a-4c**. Results are expressed as mean \pm SD of 2 independent experiments with at least six replicates.

In vitro BNCT

To evaluate the potential of the compounds **9**, **4a-4c** as BNCT agents their cytotoxic activities towards U87 cells were tested after neutron irradiation for 5 h at room temperature. Compounds were added at equimolar concentration of 200 μM . The cellular viability was determined by the MTT assay after 24 h incubation in compound free medium. The viability of cells after neutron irradiation in the presence or absence of the tested compounds was compared to that observed in controls (cells only). As can be seen in Fig. 3, neutron irradiation induced an increase in the cytotoxic effect in particular for compound **4a**.

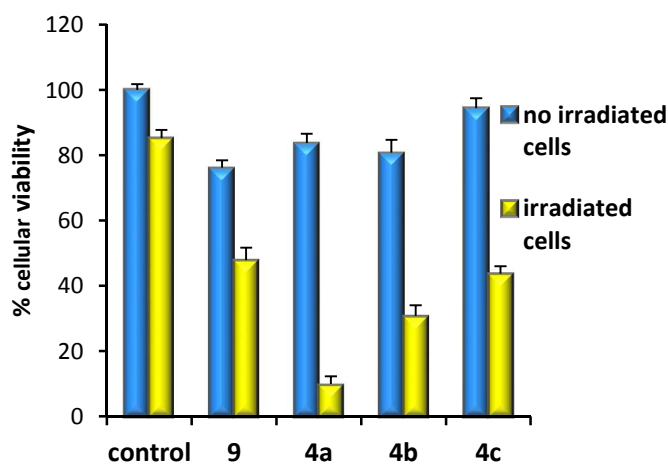


Fig. 3 Cellular viability (%) of U87 cells after neutron irradiation. Cells with or without compounds were irradiated at room temperature for 5 h at nominal thermal neutron fluence rate 6.6×10^7 neutrons $\text{cm}^{-2} \text{s}^{-1}$, 1 MW. After irradiation cellular viability was evaluated by the MTT assay.

Results as mean \pm SD of 2 independent experiments show a significant cytotoxic effect induced by neutron irradiation in particular for compound **4a**.

Cellular distribution by ICP-MS

As can be observed from Fig. 4, comparative cellular distribution studies of compounds **9**, **4a-4c** with the U87 cells were conducted in order to determine the boron content delivered by the compounds. The boron content was determined by inductively-coupled plasma mass spectroscopy (ICP-MS) in the cytosol, membrane/particulate, nucleus and cytoskeletal fractions isolated from cells after 6 h exposure to the compounds at 200 μM . Thus, treatment of cells with compounds showed that total boron content is similar for all compounds with exception of **4c**. Moreover, the amount of boron localized in the membrane and cytoskeletal fractions represent about 80% (**4a**) and more than 90% (**9**, **4b** and **4c**) of total boron taken up by cells. The uptake in the nucleus was small; the highest value found was 4.6% for **4a**. In addition compound **4a** present higher uptake in the cytosol.

This result indicates that compounds can target cellular components present mainly at the membrane or cytoskeleton, however without a cytotoxic effect, a factor that are critical in the design of new agents for BNCT. Moreover the concentration of boron deposited into the cell is adequate for this therapeutic modality. We calculated an uptake of approx. 1.4×10^{11} B atoms and consequently 2.8×10^{10} ^{10}B atoms per cell, an amount superior to the recommended concentration of 10^8 - 10^9 ^{10}B atoms.²⁵

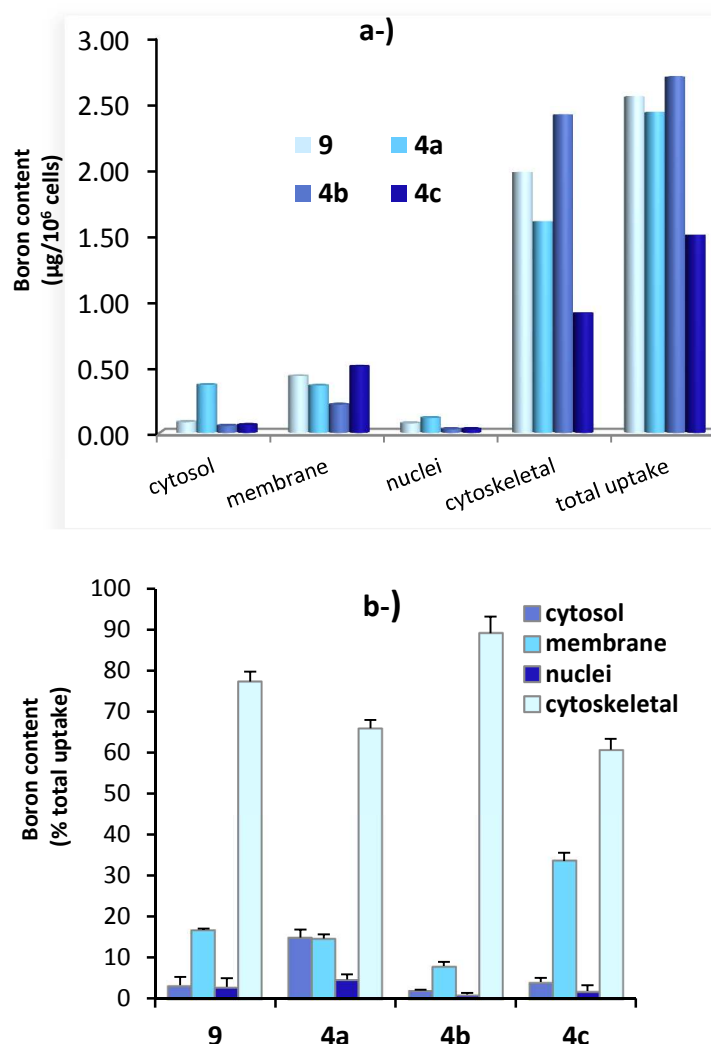


Fig. 4 The subcellular distribution (boron content) of the carboranyl methylacridones into the U87 cells. Cells were incubated with the compounds at 200 μM for 6 h challenge. The cytosol, membrane/particulate, nuclear and cytoskeletal fractions were extracted and their boron content was

determined by ICP-MS. Results show the boron content expressed as: a-) $\mu\text{g}/10^6$ cells and b-) percentage of total uptake (mean \pm SD of 2 independent experiments).

Cellular trafficking by fluorescence microscopy

The cellular trafficking of compounds was studied by time-lapse confocal fluorescence microscopy in live cells, by taking advantage of their fluorescent properties. Cells were previously incubated with dihydroethidium (DHE) or Hoechst 33342 for whole-cell or nuclei co-localization and imaged every minute for 30 min after addition of compounds in the medium (200 μM , final concentration). As depicted in Fig. 5 **4a** rapidly accumulates in the U87 cells but not significantly in the nucleus. Considerable accumulation of fluorescence was already evident after 15 min incubation. The accumulation of **4c** is slower but present identical features as **4a**, *i.e.*, accumulation in the cells but no visible uptake in the nucleus. The cellular trafficking of compounds **9** (absorption/emission: 387/400 nm) and **4b** (absorption/emission: 450/560 nm) was not possible to follow. The former, due to the particular excitation and emission characteristics of the compound in the UV spectra, the later, probably due to a lower fluorescence intensity. In fact, in compound **4b** there is a conjugation between the methoxyl group oxygen atoms and the benzoacridone nucleus, which means an increase on the electronic density of the benzoacridone nucleus, but the same does not occur in the case of derivative **4c** due to the steric hindrance of the bromo substituents. This effect can be observed by the chemical shift of carbon methoxyls, **4b** at 55 ppm and **4c** at 61 ppm. The presence of the dimethoxy-hydroquinone system could induce

fluorescence quenching and the presence of the halogens could counteract this effect.

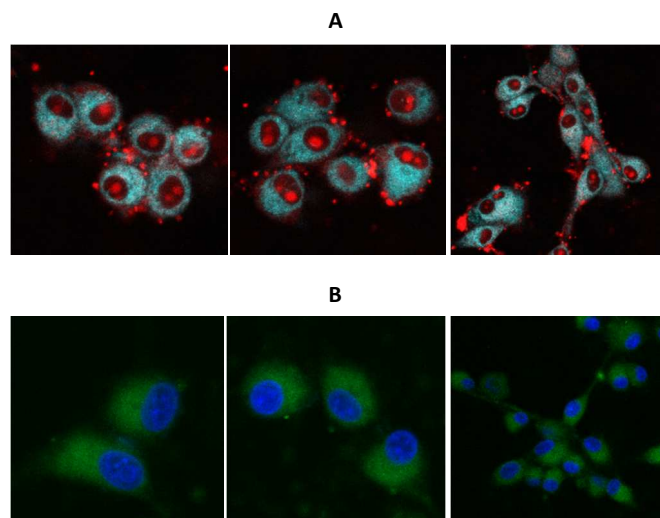


Fig. 5 Fluorescent live-cell imaging of the carboranyl-methylbenzo[*b*]acridones **4a** (A) and **4c** (B) in the U87 cells visualized by time-lapse confocal microscopy. The whole cell or cell nuclei were stained with DHE (**4a**) shown in red or Hoechst 33342 (**4c**) shown in blue. After incubation with the dyes for 10 min, the cells were washed with PBS and the compounds were added at 200 μM . Images in blue (**4a**) or green (**4c**) channels were acquired after a 30 min time period.

Ultrastructural Analysis

Results from the ultrastructural study of the cells treated with compounds **9**, **4a-4c** and after neutron irradiation are presented in Fig. 6. Micrographs showed for cells treated with compound **4a** a clear accumulation of membranous whorls in the delimiting areas of cytoplasm devoid of organelles, which correlates with the higher cytotoxic effect of this compound combined with radiation. Cells treated with the other compounds did not show significant ultrastructural alterations in comparison with the control.

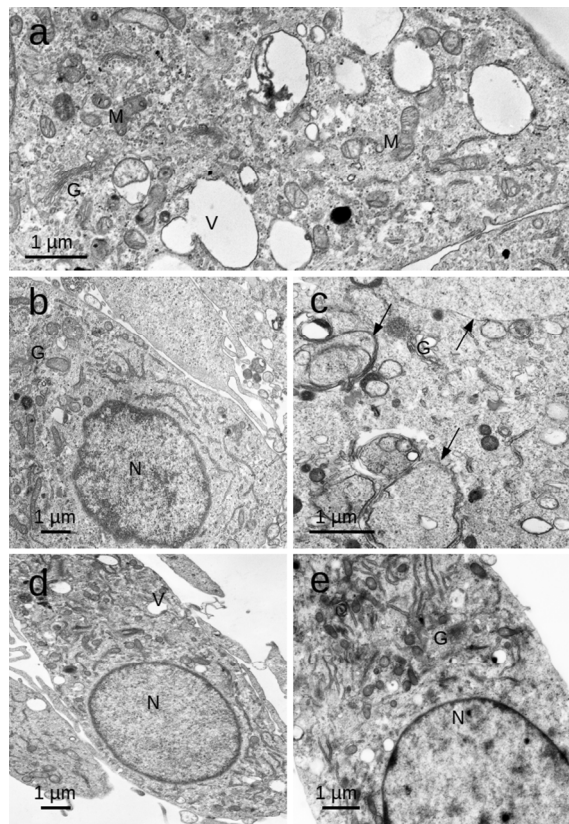


Fig. 6 Ultrastructural studies. Morphological alterations induced by compounds when combined with neutron irradiation. **a)** Control cells showing normal organelles in the cytoplasm; **b)** Cells treated with compound **9**; **c)** Cells treated with compound **4a** showing whorls of membranes sequestering areas of cytoplasm devoid of organelles (arrows); **d)** Cells treated with compound **4b**; **e)** Cells treated with compound **4c**. All cells except those treated with compound **4a** display normal ultrastructural features. N – Nucleus; M- Mitochondria; V – cytoplasmic vacuoles; G – Golgi apparatus.

Experimental

Materials

Most of the reagents used for synthesis were obtained from Sigma-Aldrich and were used without further purification. Decaborane was obtained from Alfa Aesar. Melting points were determined on a Büchi Melting Point B-540 apparatus and are uncorrected. NMR spectra were recorded on Bruker

Avance 300 (300.13 MHz for ^1H and 75.47 MHz for ^{13}C) and Bruker Avance 500 (500.13 MHz for ^1H and 125.76 MHz for ^{13}C) spectrometers, using CDCl_3 as solvent. Chemical shifts (δ) are reported in ppm values and the coupling constants (J) in Hz. The internal standard was TMS. ^{13}C assignments were made using 2D gHSQC and gHMBC (long-range C/H coupling constants were optimised to 7 Hz) experiments. Positive-ion ESI mass spectra were acquired using a Q-TOF 2 instrument [diluting 1 μL of the sample chloroform solution ($\sim 10^{-5}$ M) in 200 μL of 0.1% formic acid/methanol solution. Nitrogen was used as nebuliser gas and argon as collision gas. The needle voltage was set at 3000 V, with the ion source at 80°C and desolvation temperature at 150°C. Cone voltage was 35 V]. High resolution mass spectra (HRMS-ESI $^+$) were performed on a microTOF (focus) mass spectrometer. Ions were generated using an Apollo II (ESI) source. Ionization was achieved by electrospray, using a voltage of 4500 V applied to the needle, and a counter voltage between 100 and 150 V applied to the capillary. Preparative thin layer chromatography was carried out with Riedel silica gel 60 DGF254, and column chromatography using Acros silica gel 60, 35-70 μm .

Synthesis and characterization

7-(Prop-2-yn-1-yl)benzo[*b*]acridin-12(7*H*)-ones **2a-c** and 10-(prop-2-yn-1-yl)acridin-9(10*H*)-one (**7**)

A solution of the appropriate acridone **1a-c** or **6** (0.102 mmol), sodium hydride (4.4 mg, 0.183 mmol) and propargyl bromide (22 μL , 0.204 mmol) in dry THF (3 mL) was refluxed for 2 h (derivative **1a**), 2.5 h (derivative **1b**) and 4 h

(derivative **1c** and **6**). After this period light petroleum (5 mL) was added and the reaction mixture was refluxed for more 30 minutes.

The mixture was extracted with AcOEt (2 x 30 mL), and dried over Na₂SO₄. The residue obtained after concentration of the solvent was purified by flash column chromatography over silica gel using light petroleum:AcOEt (1:1) as eluent.

7-(Prop-2-yn-1-yl)benzo[b]acridin-12(7H)-one (2a)

Yellow solid (24.8 mg, 86%); m.p. 261-262 °C; ¹H NMR (300.13 MHz, CDCl₃): δ = 2.45 (t, 1H, *J* 2.4 Hz, H-3'), 5.13 (d, 2H, *J* 2.4 Hz, H-1'), 7.32 (dd, 1H, *J* 7.2, 7.7 Hz, H-10), 7.47 (ddd, 1H, *J* 1.6, 7.2, 8.3 Hz, H-3), 7.58 (d, 1H, *J* 8.4 Hz, H-8), 7.61 (ddd, 1H, *J* 1.1, 7.2, 8.3 Hz, H-4), 7.80 (ddd, 1H, *J* 1.6, 7.2, 8.4 Hz, H-9), 7.91 (s, 1H, H-6), 7.97 (d, 1H, *J* 8.3 Hz, H-5), 8.08 (d, 1H, *J* 8.3 Hz, H-2), 8.57 (dd, 1H, *J* 1.6, 7.7 Hz, H-11), 9.14 (s, 1H, H-1); ¹³C NMR (75.47 MHz, CDCl₃): δ = 37.1 (C-1'), 73.8 (C-3'), 77.6 (C-2'), 110.4 (C-6), 114.3 (C-8), 121.2 (C-10), 121.6 (C-11a), 122.7 (C-12a), 124.8 (C-3), 127.1 (C-5), 128.2 (C-11), 128.3 (C-1a), 128.9 (C-4), 129.3 (C-1), 129.6 (C-2), 134.8 (C-9), 136.5 (C-5a), 138.8 (C-6a), 142.7 (C-7a), 179.4 (C-12); ESI⁺-MS *m/z* (%) = 284 (100) [M+H]⁺, 306 (21) [M+Na]⁺, 589 (68) [2M+Na]⁺, 872 (4) [3M+Na]⁺; HRMS-ESI⁺ *m/z* for C₂₀H₁₄NO calcd 284.1070; found 284.1066.

2,5-Dimethoxy-7-(prop-2-yn-1-yl)benzo[b]acridin-12(7H)-one (2b)

Yellow solid (26.3 mg, 75%); m.p. 285-286 °C; ¹H NMR (300.13 MHz, DMSO-*d*₆): δ = 3.46 (t, 1H, *J* 2.2 Hz, H-3'), 4.00 and 4.01 (s, 6H, 2,5-OCH₃), 5.36 (d, 2H, *J* 2.2 Hz, H-1'),

6.81 (d, 1H, *J* 8.4 Hz, H-3), 7.01 (d, 1H, *J* 8.4 Hz, H-4), 7.35 (ddd, 1H, *J* 0.7, 6.7, 7.9 Hz, H-10), 7.82 (d, 1H, *J* 8.5 Hz, H-8), 7.90 (ddd, 1H, *J* 1.7, 6.7, 8.5 Hz, H-9), 8.28 (s, 1H, H-6), 8.36 (dd, 1H, *J* 1.7, 7.9 Hz, H-11), 9.20 (s, 1H, H-1); ¹³C NMR (75.47 MHz, DMSO-*d*₆): δ = 36.2 (C-1'), 55.7 and 55.9 (2,5-OCH₃), 75.9 (C-3'), 78.6 (C-2'), 101.8 (C-3), 105.7 (C-6), 106.5 (C-4), 115.6 (C-8), 120.7, 120.8 and 121.3 (C-1a, C-11a and C-12a), 121.4 (C-10), 122.4 (C-1), 127.1 (C-11), 129.0 (C-5a), 135.1 (C-9), 138.3 (C-6a), 142.2 (C-7a), 147.7 (C-5), 149.7 (C-2), 177.8 (C-12); ESI⁺-MS *m/z* (%) = 344 (100) [M+H]⁺, 366 (6) [M+Na]⁺, 709 (38) [2M+Na]⁺; HRMS-ESI⁺ *m/z* for C₂₂H₁₈NO₃ calcd 344.1281; found 344.1277.

3,4-Dibromo-2,5-dimethoxy-7-(prop-2-yn-1-yl)benzo[b]acridin-12(7H)-one (2c)

Yellow solid (38.8 mg, 76%); m.p. 269-270 °C; ¹H NMR (300.13 MHz, CDCl₃): δ = 2.45 (t, 1H, *J* 2.3 Hz, H-3'), 4.08 and 4.09 (s, 6H, 2,5-OCH₃), 5.15 (d, 2H, *J* 2.3 Hz, H-1'), 7.35 (dd, 1H, *J* 7.3, 7.7 Hz, H-10), 7.59 (d, 1H, *J* 8.8 Hz, H-8), 7.82 (ddd, 1H, *J* 1.7, 7.3, 8.8 Hz, H-9), 8.16 (s, 1H, H-6), 8.56 (dd, 1H, *J* 1.7, 7.7 Hz, H-11), 9.33 (s, 1H, H-1); ¹³C NMR (75.47 MHz, CDCl₃, chemical shifts assigned based on HSQC and HMBC projections): δ = 36.9 (C-1'), 61.5 (2,5-OCH₃), 73.7 (C-3'), 78.4 (C-2'), 105.9 (C-6), 114.6 (C-8), 115.3 (C-3), 119.0 (C-4), 121.7 (C-10), 122.0 (C-11a), 123.3 (C-1a and C-12a), 124.9 (C-1), 128.1 (C-11), 130.9 (C-5a), 135.1 (C-9), 139.7 (C-6a), 142.6 (C-7a), 150.2 (C-5), 152.6 (C-2), 178.9 (C-12); ESI⁺-MS *m/z* (%) = 500 (50) ([M+H]⁺, ⁷⁹Br, ⁷⁹Br), 502 (100) ([M+H]⁺, ⁷⁹Br, ⁸¹Br), 504 (47) ([M+H]⁺,

^{81}Br , ^{81}Br); HRMS-ESI⁺ m/z for $\text{C}_{22}\text{H}_{16}^{79}\text{Br}_2\text{NO}_3$ calcd 141.7 (C-4a and C-4b), 178.1 (C-9); ESI⁺-MS m/z (%) = 234 499.9492; found 499.9485; for $\text{C}_{22}\text{H}_{16}^{79}\text{Br}^{81}\text{BrNO}_3$ calcd (100) [M+H]⁺, 256 (37) [M+Na]⁺, 489 (13) [2M+Na]⁺; 501.9471; found 501.9465; for $\text{C}_{22}\text{H}_{16}^{81}\text{Br}_2\text{NO}_3$ calcd HRMS-ESI⁺ m/z for $\text{C}_{16}\text{H}_{12}\text{NO}$ calcd 234.0913; found 503.9450; found 503.9445. 234.0910.

7-(Propa-2-dien-1-yl)benzo[*b*]acridin-12(7*H*)-one (3)

Yellow solid (4.3 mg, 15%); m.p. 262-263°C; ¹H NMR (300.13 MHz, CDCl₃): δ = 5.47 (d, 2H, *J* 6.3 Hz, H-3'), 6.68 (t, 1H, *J* 6.3 Hz, H-1'), 7.27-7.31 (m, 1H, H-10), 7.45 (ddd, 1H, *J* 1.3, 6.7, 8.4 Hz, H-3), 7.58 (ddd, 1H, *J* 1.3, 6.7, 8.3 Hz, H-4), 7.71-7.73 (m, 2H, H-8 and H-9), 7.92 (d, 1H, *J* 8.3 Hz, H-5), 8.03 (s, 1H, H-6), 8.07 (d, 1H, *J* 8.4 Hz, H-2), 8.56 (dd, 1H, *J* 1.6, 8.0 Hz, H-11), 9.14 (s, 1H, H-1); ¹³C NMR (75.47 MHz, CDCl₃): δ = 83.4 (C-3'), 95.5 (C-1'), 112.1 (C-6), 115.9 (C-8), 121.0 (C-11a), 121.1 (C-10), 122.2 (C-12a), 124.6 (C-3), 127.0 (C-5), 127.9 (C-11), 128.4 (C-1a), 128.6 (C-4), 129.0 (C-1), 129.6 (C-2), 134.2 (C-9), 136.2 (C-5a), 138.9 (C-6a), 142.8 (C-7a), 179.2 (C-12), 210.1 (C-2'); ESI⁺-MS m/z (%) = 284 (100) [M+H]⁺, 306 (22) [M+Na]⁺, 589 (66) [2M+Na]⁺; HRMS-ESI⁺ m/z for $\text{C}_{20}\text{H}_{14}\text{NO}$ calcd 284.1070; found 284.1066.

10-(Prop-2-yn-1-yl)acridin-9(10*H*)-one (7)

White solid (21.9 mg, 92%); m.p. 222-223 °C; ¹H NMR (300.13 MHz, CDCl₃): δ = 2.42 (t, 1H, *J* 2.5 Hz, H-3'), 5.04 (d, 2H, *J* 2.5 Hz, H-1'), 7.33 (ddd, 2H, *J* 1.0, 7.0, 8.0 Hz, H-2, H-7), 7.59 (d, 2H, *J* 8.6 Hz, H-4, H-5), 7.77 (ddd, 2H, *J* 1.7, 7.0, 8.6 Hz, H-3, H-6), 8.55 (dd, 2H, *J* 1.7, 8.0 Hz, H-1, H-8); ¹³C NMR (75.47 MHz, CDCl₃): δ = 36.8 (C-1'), 73.8 (C-3'), 77.4 (C-2'), 114.5 (C-4 and C-5), 121.8 (C-2 and C-7), 122.7 (C-8a and C-9a), 127.9 (C-1 and C-8), 134.1 (C-3 and C-6),

10-(Propa-1,2-dien-1-yl)acridin-9(10*H*)-one (8)

White solid (6.4 mg, 27%); m.p. 221-222 °C; ¹H NMR (300.13 MHz, CDCl₃): δ = 5.42 (d, 2H, *J* 6.3 Hz, H-3'), 6.60 (t, 1H, *J* 6.3 Hz, H-1'), 7.28-7.34 (m, 2H, H-2, H-7), 7.69-7.71 (m, 4H, H-3, H-4, H-5, H-6), 8.55 (ddd, 2H, *J* 0.8, 1.4, 8.1 Hz, H-1, H-8); ¹³C NMR (75.47 MHz, CDCl₃): δ = 83.4 (C-3'), 95.3 (C-1'), 116.2 (C-4 and C-5), 121.8 (C-2 and C-7), 122.2 (C-8a and C-9a), 127.6 (C-1 and C-8), 133.5 (C-3 and C-6), 141.9 (C-4a and C-4b), 178.0 (C-9), 209.9 (C-2'); ESI⁺-MS m/z (%) = 234 (100) [M+H]⁺, 256 (7) [M+Na]⁺, 272 (2) [M+K]⁺; HRMS-ESI⁺ m/z for $\text{C}_{16}\text{H}_{12}\text{NO}$ calcd 234.0913; found 234.0911.

7-Carboranylmethylbenzo[*b*]acridin-12(7*H*)-ones 4a-c and 7-carboranylmethylacridin-9(10*H*)-one (9)

A solution of decaborane (32.2 mg, 0.264 mmol) in acetonitrile (345 μL, 0.660 mmol) and toluene (700 μL for derivatives **2a**, **2b** and **7** or 1000 μL for derivative **2c**) was refluxed for 1 h. Then the appropriated acridone **2a-c** or **7** (0.176 mmol) was added and the reaction mixture refluxed for 2 h (derivative **2a**, **2b**) or 4 h (derivative **2c** and **7**). The reaction was finished by adding 10 mL of methanol to destroy the excess of decaborane. After cooling, the solvent was evaporated and the residue purified by preparative thin layer chromatography using a mixture of light petroleum:AcOEt (4:1) as eluent.

7-Carboranylmethylbenzo[*b*]acridin-12(7*H*)-one (4a)

Yellow solid (37.4 mg, 53%); m.p. 304-305 °C; ¹H NMR (300.13 MHz, CDCl₃): δ = 0.95-3.32 (m, 10H, BH-carb), 3.68 (br-s, 1H, H-3'), 5.25 (AB, 1H, *J* 17.3 Hz, H-1'_a), 5.35 (AB, 1H, *J* 17.3 Hz, H-1'_b), 7.38 (dd, 1H, *J* 7.2, 7.6 Hz, H-10), 7.50 (d, 1H, *J* 8.7 Hz, H-8), 7.53 (ddd, 1H, *J* 1.0, 6.8, 8.2 Hz, H-3), 7.67 (ddd, 1H, *J* 1.1, 6.8, 8.3 Hz, H-4), 7.82 (ddd, 1H, *J* 1.8, 7.2, 8.7 Hz, H-9), 7.86 (s, 1H, H-6), 7.94 (d, 1H, *J* 8.3 Hz, H-5), 8.10 (d, 1H, *J* 8.2 Hz, H-2), 8.63 (dd, 1H, *J* 1.8, 7.6 Hz, H-11), 9.18 (s, 1H, H-1); ¹³C NMR (75.47 MHz, CDCl₃): δ = 48.7 (C-1'), 57.9 (C-3'), 73.0 (C-2'), 110.2 (C-6), 113.7 (C-8), 121.5 (C-11a), 122.1 (C-12a), 122.2 (C-10), 125.6 (C-3), 127.0 (C-5), 128.6 (C-1a), 129.1 (C-11), 129.5 (C-2 or C-4), 129.6 (C-2 or C-4), 130.3 (C-1), 135.1 (C-9), 136.3 (C-5a), 138.8 (C-6a), 142.6 (C-7a), 178.5 (C-12); ESI⁺-MS *m/z* (%) = 399, 400, 401, 402 (100) ([M+H]⁺, ¹⁰B₂, ¹¹B₈), 403, 404; HRMS-ESI⁺ *m/z* for C₂₀H₂₄¹⁰B₂¹¹B₈NO calcd 402.2855; found 402.2852.

2,5-Dimethoxy-7-carboranylmethylbenzo[*b*]acridin-12(7*H*)-one (4b)

Yellow solid (37.4 mg, 46%); m.p. 288-289 °C; ¹H NMR (300.13 MHz, CDCl₃): δ = 1.01-3.41 (m, 10H, BH-carb), 3.72 (br-s, 1H, H-3'), 4.02 and 4.05 (s, 6H, 2,5-OCH₃), 5.19 (AB, 1H, *J* 17.5 Hz, H-1'_a), 5.35 (AB, 1H, *J* 17.5 Hz, H-1'_b), 6.64 (d, 1H, *J* 8.3 Hz, H-3), 6.82 (d, 1H, *J* 8.3 Hz, H-4), 7.34 (dd, 1H, *J* 7.3, 7.7 Hz, H-10), 7.50 (d, 1H, *J* 8.7 Hz, H-8), 7.79 (ddd, 1H, *J* 1.7, 7.3, 8.7 Hz, H-9), 8.19 (s, 1H, H-6), 8.59 (dd, 1H, *J* 1.7, 7.7 Hz, H-11), 9.48 (s, 1H, H-1); ¹³C NMR (75.47 MHz, CDCl₃): δ = 49.2 (C-1'), 55.7 and 56.0 (2,5-OCH₃),

58.2 (C-3'), 73.2 (C-2'), 101.5 (C-3), 104.8 (C-6), 106.2 (C-4), 113.9 (C-8), 121.5 (C-11a or C-12a), 121.6 (C-11a or C-12a), 122.06 (C-1a), 122.08 (C-10), 124.9 (C-1), 128.9 (C-11), 129.5 (C-5a), 134.8 (C-9), 139.0 (C-6a), 142.6 (C-7a), 148.1 (C-5), 150.7 (C-2), 178.3 (C-12); ESI⁺-MS *m/z* (%) = 459, 460, 461, 462 (100) ([M+H]⁺, ¹⁰B₂, ¹¹B₈), 463, 464; HRMS-ESI⁺ *m/z* for C₂₂H₂₈¹⁰B₂¹¹B₈NO₃ calcd 462.3067; found 462.3062.

3,4-Dibromo-2,5-dimethoxy-7-**carboranylmethylbenzo[*b*]acridin-12(7*H*)-one (4c)**

Yellow solid (49.0 mg, 45%); m.p. 277-278 °C; ¹H NMR (300.13 MHz, CDCl₃): δ = 1.03-3.44 (m, 10H, BH-carb), 3.76 (br-s, 1H, H-3'), 4.09 and 4.10 (s, 6H, 2,5-OCH₃), 5.23 (AB, 1H, *J* 17.3 Hz, H-1'_a), 5.31 (AB, 1H, *J* 17.3 Hz, H-1'_b), 7.39 (dd, 1H, *J* 7.2, 7.6 Hz, H-10), 7.50 (d, 1H, *J* 8.7 Hz, H-8), 7.84 (ddd, 1H, *J* 1.7, 7.2, 8.7 Hz, H-9), 8.15 (s, 1H, H-6), 8.59 (dd, 1H, *J* 1.7, 7.6 Hz, H-11), 9.33 (s, 1H, H-1); ¹³C NMR (75.47 MHz, CDCl₃): δ = 49.8 (C-1'), 58.3 (C-3'), 61.5 and 62.2 (2,5-OCH₃), 72.7 (C-2'), 105.9 (C-6), 113.9 (C-8), 115.2 (C-3), 120.1 (C-4), 121.6 (C-11a), 122.7 (C-10 and C-1a or C-12a), 123.4 (C-1a or C-12a), 125.7 (C-1), 129.0 (C-11), 130.8 (C-5a), 135.3 (C-9), 140.1 (C-6a), 142.6 (C-7a), 150.0 (C-5), 152.4 (C-2), 177.9 (C-12); ESI⁺-MS *m/z* (%) = 616, 617, 618, 619, 620 (100) ([M+H]⁺, ¹⁰B₂, ¹¹B₈, ⁷⁹Br, ⁸¹Br), 621, 622, 623, 624; HRMS-ESI⁺ *m/z* for C₂₂H₂₆¹⁰B₂¹¹B₈⁷⁹Br⁸¹BrNO₃ calcd 620.1251; found 620.1253.

7-Carboranylmethyl-7,12-dihydrobenzo[*b*]acridine (5a)

White solid, (15.0 mg, 22%); m.p. 298-299 °C; ¹H NMR (300.13 MHz, CDCl₃): δ = 1.02-3.40 (m, 10H, BH-carb), 3.58

(br-s, 1H, H-3'), 4.06 (s, 2H, H-12), 4.94 (br-s, 2H, H-1'), 6.98 (d, 1H, *J* 8.0 Hz, H-8), 7.00 (dt, 1H, *J* 1.0, 8.4 Hz, H-10), 7.19-7.25 (m, 1H, H-9), 7.23 (s, 1H, H-6), 7.23 (d, 1H, *J* 8.4 Hz, H-11), 7.33 (ddd, 1H, *J* 1.4, 6.9, 8.0 Hz, H-3), 7.41 (ddd, 1H, *J* 1.4, 6.9, 8.0 Hz, H-4), 7.63 (s, 1H, H-1), 7.69 (d, 1H, *J* 8.0 Hz, H-5), 7.72 (d, 1H, *J* 8.0 Hz, H-2); ¹³C NMR (75.47 MHz, CDCl₃): δ = 33.5 (C-12), 47.7 (C-1'), 58.2 (C-3'), 75.0 (C-2'), 108.5 (C-6), 112.8 (C-8), 122.5 (C-10), 124.4 (C-3), 125.4 (C-11a), 126.2 (C-4), 126.8 (C-5), 126.9 (C-2), 127.0 (C-1 and C-12a), 127.4 (C-9), 128.8 (C-11), 130.0 (C-1a), 133.0 (C-5a), 140.2 (C-6a), 141.4 (C-7a); ESI⁺-MS *m/z* (%) = 383, 384, 385, 386 (79) ([M-H]⁺, ¹⁰B₂, ¹¹B₈, acridinium type compound), 387, 388; *m/z* (%) = 385, 386, 387, 388 (100) ([M+H]⁺, ¹⁰B₂, ¹¹B₈), 389, 390; HRMS-ESI⁺ *m/z* for C₂₀H₂₆¹⁰B₂¹¹B₈N calcd 388.3063; found 388.3061; *m/z* for C₂₀H₂₄¹⁰B₂¹¹B₈N (acridinium type compound) calcd 386.2906; found 386.2904.

2,5-Dimethoxy-7-carboranylmethyl-7,12-

dihydrobenzo[*b*]acridine (5b)

White solid (11.8 mg, 15%); m.p. 285-286 °C; ¹H NMR (300.13 MHz, CDCl₃): δ = 0.81-3.29 (m, 10H, BH-carb), 3.60 (br-s, 1H, H-3'), 3.95 and 3.97 (s, 6H, 2,5-OCH₃), 4.09 (s, 2H, H-12), 4.90 (AB, 1H, *J* 16.4 Hz, H-1'_a), 5.05 (AB, 1H, *J* 16.4 Hz, H-1'_b), 6.57 (AB, 1H, *J* 8.3 Hz, H-3), 6.66 (AB, 1H, *J* 8.3 Hz, H-4), 6.98-7.02 (m, 2H, H-8, H-10), 7.20-7.24 (m, 2H, H-9, H-11), 7.65 (s, 1H, H-6), 8.01 (s, 1H, H-1); ¹³C NMR (75.47 MHz, CDCl₃): δ = 33.4 (C-12), 47.6 (C-1'), 55.7 and 55.8 (2,5-OCH₃), 58.1 (C-3'), 75.0 (C-2'), 101.5 (C-3), 102.8 (C-6), 103.4 (C-4), 112.6 (C-8), 121.6 (C-1), 122.2 (C-

10), 122.4 (C-1a), 125.0 (C-11a), 125.8 (C-5a), 126.0 (C-12a), 127.3 (C-9), 128.8 (C-11), 140.1 (C-6a), 141.3 (C-7a), 148.6 (C-5), 149.1 (C-2); ESI⁺-MS *m/z* (%) = 443, 444, 445, 446 (100) ([M-H]⁺, ¹⁰B₂, ¹¹B₈, acridinium type compound), 447, 448; HRMS-ESI⁺ *m/z* for C₂₂H₂₈¹⁰B₂¹¹B₈NO₂ (acridinium type compound) calcd 446.3118; found 446.3112.

3,4-Dibromo-2,5-dimethoxy-7-carboranylmethyl-7,12-dihydrobenzo[*b*]acridine (5c)

White solid (20.2 mg, 19%); m.p. 262-263 °C; ¹H NMR (500.13 MHz, CDCl₃): δ = 1.38-3.17 (m, 10H, BH-carb), 3.61 (br-s, 1H, H-3'), 3.98 and 3.99 (s, 6H, 2,5-OCH₃), 4.06-4.17 (m, 2H, H-12), 4.93 (AB, 1H, *J* 16.8 Hz, H-1'_a), 5.02 (AB, 1H, *J* 16.8 Hz, H-1'_b), 7.01 (d, 1H, *J* 8.2 Hz, H-8), 7.06 (t, 1H, *J* 7.4 Hz, H-10), 7.24-7.27 (m, 2H, H-9, H-11), 7.50 (s, 1H, H-6), 7.89 (s, 1H, H-1); ¹³C NMR (75.47 MHz, CDCl₃): δ = 33.5 (C-12), 47.8 (C-1'), 58.2 (C-3'), 61.3 and 61.6 (2,5-OCH₃), 74.5 (C-2'), 103.3 (C-6), 112.8 (C-8), 113.8 (C-3 or C-4), 116.4 (C-3 or C-4), 122.3 (C-1), 122.9 (C-10), 124.4 (C-1a), 124.6 (C-11a), 127.6 (C-9 or C-11), 127.8 (C-5a), 128.3 (C-12a), 128.9 (C-9 or C-11), 140.7 (C-7a), 141.5 (C-6a), 150.0 (C-5), 150.6 (C-2); ESI⁺-MS *m/z* (%) = 600, 601, 602, 603, 604 (100) ([M-H]⁺, ¹⁰B₂, ¹¹B₈, ⁷⁹Br, ⁸¹Br, acridinium type compound), 605, 606, 607, 608; HRMS-ESI⁺ *m/z* for C₂₂H₂₆¹⁰B₂¹¹B₈⁷⁹Br⁸¹BrNO₂ (acridinium type compound) calcd 604.1301; found 604.1302.

10-Carboranylmethylacridin-9(10*H*)-one (9)

White solid (39.0 mg, 63%); m.p. 278-279 °C; ¹H NMR (300.13 MHz, CDCl₃): δ = 1.12-3.45 (m, 10H, BH-carb), 3.62 (br-s, 1H, H-3'), 5.22 (s, 2H, H-1'), 7.40 (dd, 2H, *J* 7.3, 7.8

Hz, H-2, H-7), 7.51 (d, 2H, J 8.7 Hz, H-4, H-5), 7.80 (ddd, 2H, J 1.7, 7.3, 8.7 Hz, H-3, H-6), 8.61 (dd, 2H, J 1.7, 7.8 Hz, H-1, H-8); ^{13}C NMR (75.47 MHz, CDCl_3): δ = 48.4 (C-1'), 58.1 (C-3'), 72.9 (C-2'), 114.0 (C-4 and C-5), 122.6 (C-8a and C-9a), 122.8 (C-2 and C-7), 128.8 (C-1 and C-8), 134.5 (C-3 and C-6), 141.7 (C-4a and C-4b), 177.4 (C-9); ESI^+ -MS m/z (%) = 349, 350, 351, 352 (100) ($[\text{M}+\text{H}]^+$, $^{10}\text{B}_2$, $^{11}\text{B}_8$), 353, 354; HRMS- ESI^+ m/z for $\text{C}_{16}\text{H}_{22}^{10}\text{B}_2^{11}\text{B}_8\text{NO}$ calcd 352.2699; found 352.2695.

10-Carboranylmethyl-9,10-dihydroacridine (10)

White solid (8.9 mg, 15%); m.p. 257-258 °C; ^1H NMR (300.13 MHz, CDCl_3): δ = 1.00-3.30 (m, 10H, BH-carb), 3.55 (br-s, 1H, H-3'), 3.91 (s, 2H, H-9), 4.83 (s, 2H, H-1'), 6.93-7.01 (m, 4H, H-2, H-4, H-5, H-7), 7.17-7.27 (m, 4H, H-1, H-3, H-6, H-8); ^{13}C NMR (75.47 MHz, CDCl_3): δ = 33.0 (C-9), 47.4 (C-1'), 57.9 (C-3'), 75.0 (C-2'), 112.5 (C-4 and C-5), 122.4 (C-2 and C-7), 125.0 (C-8a and C-9a), 127.2 (C-3 and C-6), 128.8 (C-1 and C-8), 141.3 (C-4a and C-4b); ESI^+ -MS m/z (%) = 333, 334, 335, 336 (100) ($[\text{M}-\text{H}]^+$, $^{10}\text{B}_2$, $^{11}\text{B}_8$, acridinium type compound), 337, 338; HRMS- ESI^+ m/z for $\text{C}_{16}\text{H}_{22}^{10}\text{B}_2^{11}\text{B}_8\text{N}$ (acridinium type compound) calcd 336.2750; found 336.2745.

Cell studies

Cell culture and cellular viability

U87 human glioblastoma multiforme cell lines (American Type Culture Collection, ATCC) were cultured in DMEM with GlutaMax I (Gibco) containing 10% fetal bovine serum and 1% antibiotics in a humidified atmosphere (95% air/5% CO_2) at 37°C. The cytotoxic activity of the boron compounds

was determined using the MTT assay {MTT = [3-(4,5-dimethylthiazol-2-yl)-2,5-diphenyltetrazolium bromide]}.⁴³ For this purpose, cells (10^4 cells/well) were seeded in growth media in 96-well plates. After 24 h, the media was replaced and cells incubated with the compounds in aliquots of 200 μL /well. Compounds were first solubilized in DMSO and then in medium, and added to final concentrations from 5 μM to 200 μM . The final concentration of DMSO in cell culture medium did not exceed 1%. After continuous exposure for 6 h at 37°C, the medium was discarded and cells incubated with 200 μL of MTT solution in PBS (0.5 mg/mL) for further 3–4 h at 37°C/5% CO_2 . Then, the solution was removed and the formazan crystals formed inside the cells dissolved in 200 μL DMSO. The cellular viability was evaluated by comparing the absorbance of the resulting solutions at 570 nm for the treated cells with the absorbance for non-treated cells in a multi-well plate spectrophotometer (PowerWave Xs, Bio-Tek Instruments, USA). The cytotoxic activity of the compounds was quantified by calculating the drug concentration inhibiting tumour cell growth by 50% (IC_{50}), based on non-linear regression analysis of dose response data (GraphPad Prism software).

All compounds were tested in, at least, two independent experiments, each comprising eight replicates per concentration.

Dosimetry

The Portuguese Research Reactor (RPI) was used as neutron source for *in vitro* cell irradiations. Neutron irradiation was carried out at the vertical access of the thermal column of the

RPI, consisting of a graphite stacking that moderates the fission neutrons. Cell irradiations are performed on top of the graphite using an experimental design similar to that described by others.^{44,45} The radiation field at the irradiation facility was calculated using a general-purpose Monte Carlo code for radiation transport simulation and a detailed model which included a validated model of the reactor core.⁴⁶ The calculated neutron energy distribution was further adjusted via the multiple-foil activation method and standard unfolding codes. The intensity of the neutron beam varies with the distance from the core, i.e., is constant (within $\pm 3\%$) in the parallel direction and decreases with increasing distance with a larger relative contribution of thermal neutrons as more graphite is traversed. The conventional thermal neutron fluence rate (ϕ_0) at the highest intensity position is 6.6×10^7 neutron $\text{cm}^{-2} \text{s}^{-1}$ at 1 MW reactor power; the ratio between the epithermal neutron fluence rate per unit lethargy (θ) and ϕ_0 varies between 0.03% and 0.05% in the cell flasks location. The contribution of epithermal neutrons to the dose received by the boron loaded cells is therefore negligible.

Regarding photon doses, low neutron sensitivity thermoluminescent dosimeters of $\text{Al}_2\text{O}_3:\text{Mg},\text{Y}$ were used to evaluate the accuracy of the photon simulations and measure the photon dose itself. It was concluded that the major (>99%) contribution to the photon dose are neutron interactions with the facility materials, therefore a direct relation between photon dose and thermal neutron fluence can be derived. Details on the procedures may be found in.⁴⁷

The neutron fluence and photon dose received by the cells in the actual irradiation was monitored using pure gold foils underneath the cell flasks. The ratio of the foil response to the thermal and epithermal neutron fluence rates and to the photon dose rate was previously determined in a calibration run.

In vitro cell neutron irradiation

Prior to irradiation, the cells in culture flasks at a density of approximately 10^6 cells/5mL medium were pre-incubated for 1 h with the compounds at a concentration of 200 μM in medium. Thereafter the cells were irradiated at room temperature for 5 h at 1 MW reactor power. The conventional thermal neutron fluence and the photon dose imparted to the cells during the irradiation were 6.6×10^7 n $\text{cm}^{-2} \text{s}^{-1}$ and 720 mGy, respectively. The maximum discrepancy between the measurements and this reported value is 17% due to the neutron fluence gradient within the irradiation facility.

Exponentially growing U87 cells were distributed in the following groups: 1) untreated cells without neutrons; 2) cells + neutrons; 3) cells with the compounds at 200 μM without neutrons; 4) cells with the compounds at 200 μM + neutrons. Cells that have not been treated with the boron compounds were used as controls. Following irradiation, the cells were placed in boron free medium in a humidified atmosphere containing 5% CO_2 at 37°C. After 24 h the cellular viability was evaluated by the MTT assay. The absorbance of the resulting solutions was measured at 570 nm with a Varian DMS 80 UV-Vis spectrophotometer.

Boron analysis by ICP-MS

The total cellular boron content was analysed by a Thermo X-Series Quadrupole inductively coupled plasma mass spectrometer (ICP-MS). U87 cells (approx. 10^6 cells/5 mL medium) were exposed to the compounds at 200 μ M for 6 h at 37°C, then washed with ice-cold PBS and centrifuged to obtain a cellular pellet. The cytosol, membrane/particulate, cytoskeletal and nuclear fractions were extracted using a FractionPREPTM, cell fractionation system (BioVision, USA) and performed according to the manufacturer's protocol. The boron content in the different fractions were measured after digestion of the samples in a closed pressurized microwave digestion unit (Mars5, CEM) with medium pressure HP500 vessels and then diluted in ultrapure water to obtain 2.0% (v/v) nitric acid. The instrument was tuned using a multielement ICP-MS 71 C standard solution (Inorganic Venture). Indium (¹¹⁵In) at 10 mM was used as internal standard.

Uptake by fluorescence microscopy

Cellular uptake of compounds **4a** and **4c** was visualized by performing time-lapse confocal microscopy imaging of live U87 cells. Briefly, cells in medium (ca. 10^5 cells/mL) were seeded on sterile 35 mm Petri dishes (MatTek, Ashland, MA, USA). After 24 h incubation at 37°C, cells were labelled with two different fluorescent dyes (Molecular Probes, Eugene, OR, USA) dehydroethidium (DHE) (λ_{ex} 500; λ_{em} 600) for compound **4a** (λ_{ex} 453; λ_{em} 507) or Hoechst 33342 (λ_{ex} 350; λ_{em} 480) for compound **4c** (λ_{ex} 464; λ_{em} 518) at 1 μ g/mL for 5 min at 37°C. DHE freely permeates cell membranes and inside the cell is oxidized to ethidium bromide (red

fluorescence). After labelling, the cells were washed and maintained in DMEM/F12 without phenol red for live imaging experiments. Cells were imaged with a Zeiss LSM 510 META inverted laser scanning confocal microscope (Carl Zeiss, Germany) fitted with a large incubator for 37°C (Pecon, Germany) with use of a PlanApochromat 63/1.4 oil-immersion objective. Ethidium bromide fluorescence was detected by use of the 514 nm laser line of an argon laser (45 mW nominal output) and a 530-600 nm band-pass filter. Hoechst fluorescence was detected using a Diode 405 nm laser (50 mW nominal output) and a 420-480 nm band-pass filter. The fluorescence of **4a** was detected using the 420-480 nm band-pass filter. A transmission detector (PMT) was used to provide a transmission light image of the sample by detecting the scanning 488 nm laser. The pinhole aperture was adjusted in both channels to achieve the same optical slice thickness (1 μ m). After addition of the compounds to the cells (200 μ m, final concentration) sequential images in both blue (**4a**) or green (**4c**) and red (ethidium bromide) or blue (Hoechst) channels were acquired every minute over a 30 min time period.

Ultrastructural analysis

After irradiation (cells +/- compounds + neutrons) the culture media was replaced by primary fixative (5 mL) consisting of glutaraldehyde (3%) in sodium cacodylate buffer (pH 7.3, 0.1 M). After primary fixation for 2 h at 4°C, the glutaraldehyde was replaced by sodium cacodylate buffer. Cells were scraped, pelleted, and embedded in agar (2%) for further processing. The samples were washed in cacodylate buffer

and secondarily fixed for 3 h in osmium tetroxide (1%) in sodium cacodylate buffer (pH 7.3, 0.1 M). Then samples were washed in acetate buffer (pH 5.0, 0.1 M) and further fixed in uranyl acetate (0.5%) in the same buffer for 1 h. Dehydration was carried out with increasing concentrations of ethanol. After passage through propylene oxide, the samples were embedded in Epon-Araldite, with use of SPI-Pon as an Epon 812 substitute. Thin sections were made with glass or diamond knives and stained with aqueous uranyl acetate (2%) and Reynold's lead citrate. The stained sections were studied and photographed with a JEOL 100-SX electron microscope.

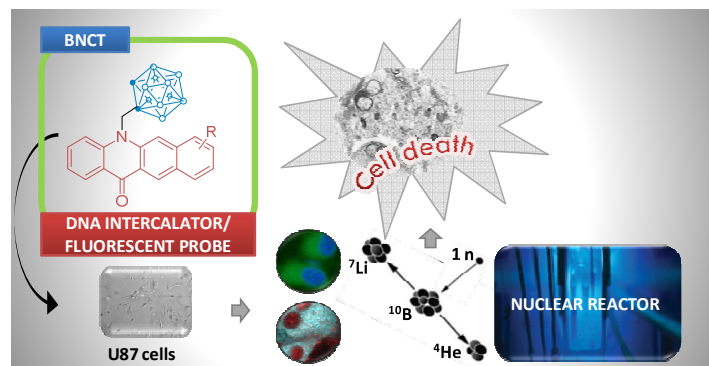
Conclusions

Glioblastoma has long been the focus of BNCT research due to its radioresistance and infiltrative growth pattern. Clinical and experimental BNCT using BSH and BPA has shown potential but no proven therapeutic advantages. Research is therefore justified to further evaluate this experimental treatment modality. Recent literature discussed some of more recent results and progress in BNCT providing hope for this unique and exciting mode of clinical therapy.⁴⁸

Two criteria must be fulfilled for clinical application of BNCT: an adequate source of high flux thermal neutrons along with a boron carrier that is able to concentrate in glioma cells and tissues. High concentration of boron within tumour cell should be obtained in order to maximize the therapeutic effect.

In this study a series of four acridone and benzo[*b*]acridone derivatives bearing carboranyl moieties have been synthesized, characterized and evaluated for new BNCT

agents using the U87 human glioblastoma cells. The compounds enters the cells and deposited an adequate amount of B atoms (2.8×10^{10} ^{10}B atoms per cell) superior to the recommended concentration of 10^8 - 10^9 ^{10}B atoms.²⁴ The compounds also fulfilled the requirement of a low cytotoxicity. Remarkable was the fact that compound **4a**, carboranylmethylbenzo[*b*]acridin-12(7*H*)-one presented considerably high activity in the U87 cells if combined with neutron irradiation. Therefore, although further studies need to be done, this set of results suggests that compound **4a** may be considered as lead compound for a new generation of BNCT agents although implications for therapy applications are at present obviously only exploratory. We found the RPI an excellent facility to conduct *in vitro/in vivo* experiments and we consider that a standard protocol for further trials had been created.



Graphical abstract Acridone derivatives bearing carboranyl moieties as fluorescent probes for boron neutron capture therapy (BNCT) of the glioblastoma.

Acknowledgements

Thanks are due to the University of Aveiro, Portuguese Foundation for Science and Technology (FCT), European Union, QREN, FEDER and COMPETE for funding the QOPNA research unit (project PEst-C/QUI/UI0062/2013) and the Portuguese NMR Network. A.F.F. Silva and R.S.G.R. Seixas thank project PEst-C/QUI/UI0062/2013, QOPNA and FCT for their grants (BI/UI51/5615/2011 and SFRH/BPD/74282/2010, respectively).

Notes

^aDepartamento de Química-QOPNA and ^{a§}Laboratório Central de Análises, Universidade de Aveiro, 3810-193 Aveiro, Portugal

^bCentro de Ciências e Tecnologias Nucleares and ^{yb}Laboratório de Engenharia Nuclear, Instituto Superior Técnico, Universidade de Lisboa, Estrada Nacional 10 (km 139.7) 2695-066 Bobadela LRS, Portugal

e-mail: fmarujo@ctn.ist.utl.pt; **Tel:** (+)351219946225; **Fax:** (+)351219550117

^cCentro de Investigação Interdisciplinar Egas Moniz, Quinta da Granja, Monte da Caparica 2829-511, Caparica, Portugal and CESAM-Lisboa, Faculdade de Ciências da Universidade de Lisboa, Campo Grande, 1749-016 Lisboa, Portugal

^dFaculdade de Medicina da Universidade de Lisboa, Instituto Medicina Molecular, Av. Prof. Egas Moniz, 1649-028 Lisboa Portugal

References

- 1 A. Omuro and L. M. DeAngelis. Glioblastoma and other malignant gliomas: a clinical review. *JAMA*, 2013, **310**, 1842-1850.

- 2 M. M. Mrugala. Advances and challenges in the treatment of glioblastoma: a clinician's perspective. *Discov. Med.*, 2013, **15**, 221-230.
- 3 C. Caruso, M. Carcaterra and V. Donato. Role of radiotherapy for high grade gliomas management. *J. Neurosurg. Sci.*, 2013, **57**, 163-169.
- 4 C. P. Tanase, A. M. Enciu, S. Mihai, A. I. Neagu, B. Calenic and M. L. Cruceru. Anti-cancer Therapies in High Grade Gliomas. *Curr. Proteomics*, 2013, **10**, 246-260.
- 5 R. F. Barth, J. A. Coderre, M. G. Vicente and T. E. Blue. Boron neutron capture therapy of cancer: current status and future prospects. *Clin Cancer Res*, 2005, **11**, 3987-4002.
- 6 R. F. Barth. Boron neutron capture therapy at the crossroads: challenges and opportunities. *Appl. Radiat. Isot.*, 2009, **67**, S3-S6.
- 7 T. Yamamoto, K. Nakai, A. Matsumura. Boron neutron capture therapy for glioblastoma. *Cancer Lett.*, 2008, **262**, 143-152.
- 8 M. A. Pisarev, M. A. Dagrosa and G. J. Juvenal. Boron neutron capture therapy in cancer: past, present and future. *Arq. Bras. Endocrinol. Metabol.*, 2007, **51**, 852-856.
- 9 S. Altieri, S. Bortolussi, R. F. Barth, L. Roveda and A. Zonta. Thirteenth International Congress on Neutron Capture Therapy. *Appl. Radiat. Isot.*, 2009, **67**, S1-S2.

- 10 T. Kageji, Y. Mizobuchi, S. Nagahiro, Y. Nakagawan and Kumada H. Clinical results of boron neutron capture therapy (BNCT) for glioblastoma. *Appl. Radiat. Isot.*, 2011, **69**, 1823-1825.
- 11 R. F. Barth, A. H. Soloway and R. M. Brugger. Boron neutron capture therapy of brain tumors: past history, current status, and future potential. *Cancer Invest.*, 1996, **14**, 534-550.
- 12 D. R. Lu, S. C. Mehta and W. Chen. Selective boron drug delivery to brain tumors for boron neutron capture therapy. *Adv. Drug Deliv. Rev.*, 1997, **26**, 231-247.
- 13 A. H. Soloway, R. F. Barth, R. A. Gahbauer, T. E. Blue and J. H. Goodman. The rationale and requirements for the development of boron neutron capture therapy of brain tumors. *J. Neurooncol.*, 1997, **33**, 9-18.
- 14 T. Nguyen, G. L. Brownell, S. A. Holden, S. Kahl, M. Miura and B. A. Teicher. Subcellular distribution of various boron compounds and implications for their efficacy in boron neutron capture therapy by Monte Carlo simulations. *Radiat. Res.*, 1993, **133**, 33-40.
- 15 R. Gahbauer, N. Gupta, T. Blue, J. Goodman, R. Barth, J. Grecula, A. H. Soloway, W. Sauerwein and A. Wambersie. Boron neutron capture therapy: principles and potential. *Recent Results Cancer Res.*, 1998, **150**, 183-209.
- 16 I. B. Sivaev and V. V. Bregadze. Polyhedral Boranes for Medical Applications: Current Status and Perspectives. *Eur. J. Inorg. Chem.*, 2009, 1433-1450.
- 17 C. Viñas i Teixidor. The uniqueness of boron as a novel challenging element for drugs in pharmacology, medicine and for smart biomaterials. *Future Med. Chem.*, 2013, **5**, 617-619.
- 18 C. H. Hsieh, Y. F. Chen, F. D. Chen, J. J. Hwang, J. C. Chen, R. S. Liu, J. J. Kai, C. W. Chang and H. E. Wang. Evaluation of pharmacokinetics of 4-borono-2-18F-fluoro-L-Phenylalanine for boron neutron capture therapy in a glioma-bearing rat model with hyperosmolar blood-brain barrier disruption. *J. Nucl. Med.*, 2005, **46**, 1858-1865.
- 19 A. Crivello, C. Nervi, R. Gobetto, S. G. Crich, I. Szabo, A. Barge, A. Toppino, A. Deagostino, P. Venturello and S. Aime. Towards improved boron neutron capture therapy agents: evaluation of in vitro cellular uptake of a glutamine-functionalized carborane. *J. Biol. Inorg. Chem.*, 2009, **14**, 883-890.
- 20 T. Betzel, T. Heß, B. Waser, J. C. Reubi and F. Roesch. *Closo*-Borane conjugated regulatory peptides retain high biological affinity: synthesis of *closo*-borane conjugated Tyr3-octreotate derivatives for BNCT. *Bioconjug. Chem.*, 2008, **19**, 1796-1802.
- 21 J. Bonjoch, M. G. Drew, A. González, F. Greco, S. Jawaid, H. M. Osborn, N. A. Williams and P. Yaqoob. Synthesis and evaluation of novel boron-containing complexes of potential use for the

- selective treatment of malignant melanoma. *J. Med. Chem.*, 2008, **51**, 6604-6608.
- 22 W. Yang, R. F. Barth, G. Wu, T. Huo, W. Tjarks, M. Ciesielski, R. A. Fenstermaker, B. D. Ross, C. J. Wikstrand, K. J. Riley and P. J. Binns. Convection enhanced delivery of boronated EGF as a molecular targeting agent for neutron capture therapy of brain tumors. *J. Neurooncol.*, 2009, **95**, 355-365.
- 23 R. P. Evstigneeva, A. V. Zaitsev, V. N. Luzgina, V. A. Ol'shevskaya and A. A. Shtil. Carboranylporphyrins for boron neutron capture therapy of cancer. *Curr. Med. Chem. Anticancer Agents*, 2003, **3**, 383-392.
- 24 M. W. Easson, F. R. Fronczek, T. J. Jensen, M. G. H. Vicente. Synthesis and in vitro properties of trimethylamine- and phosphonate -substituted carboranylporphyrins for application in BNCT. *Bioorg. Med. Chem.*, 2008, **16**, 3191-3208.
- 25 E. L. Crossley, E. J. Ziolkowski, J. A. Coderre and L. M. Rendina. Boronated DNA-binding compounds as potential agents for boron neutron capture therapy. *Mini-Rev Med. Chem.*, 2007, **7**, 303-313.
- 26 J. Yoo and Y. Do. Synthesis of stable platinum complexes containing carborane in a carrier group for potential BNCT agents. *Dalton Trans.*, 2009, 4978-4986.
- 27 N. P. Barry and Sadler P. J. Dicarba-closo-dodecarborane-containing half-sandwich complexes of ruthenium, osmium, rhodium and iridium: biological relevance and synthetic strategies. *Chem. Soc. Rev.*, 2012, **41**, 3264-3279.
- 28 R. L. Moss. Critical review, with an optimistic outlook, on Boron Neutron Capture Therapy (BNCT). *Appl. Radiat. Isot.*, 2013, DOI: 10.1016/j.apradiso.2013.11.109.
- 29 V. V. S. R. Prasad, G. J. Peters, C. Lemos, I. Kathmann and Y. C. Mayur. Cytotoxicity studies of some novel fluoro acridone derivatives against sensitive and resistant cancer cell lines and their mechanistic studies. *Eur. J. Pharm. Sci.*, 2011, **43**, 217-224.
- 30 A. Paul, P. Sengupta, Y. Krishnan and S. Ladame. Combining G-Quadruplex Targeting Motifs on a Single Peptide Nucleic Acid Scaffold: A Hybrid (3+1) PNA-DNA Bimolecular Quadruplex. *Chem. Eur. J.*, 2008, **14**, 8682-8689.
- 31 J. Kaur, P. Singh. ATP selective acridone based fluorescent probes for monitoring of metabolic events. *Chem. Commun.*, 2011, **47**, 4472-4474.
- 32 R. J. Harrison, A. P. Reszka, S. M. Haider, B. Romagnoli, J. Morrell, M. A. Read, S. M. Gowan, C. M. Inces, L. R. Kelland, S. Neidle. Evaluation of by disubstituted acridone derivatives as telomerase inhibitors: the importance of G-quadruplex binding. *Bioorg Med Chem Lett*, 2004, **14**, 5845-5849.
- 33 Y. Hagiwara, T. Hasegawa, A. Shoji, M. Kuwahara, H. Ozaki and H. Sawai. Acridone-tagged DNA as a new probe for DNA detection by fluorescence

- resonance energy transfer and for mismatch DNA recognition. *Bioorg. Med. Chem.*, 2008, **16**, 7013-7020.
- 34 P. Belmont and I. Dorange. Acridine/acridone: a simple scaffold with a wide range of application in oncology. *Expert Opin. Ther. Patents*, 2008, **18**, 1211-1224.
- 35 G. Cholewiński, K. Dzierzbicka and A. M. Kolodziejczyk. Natural and synthetic acridines/acridones as antitumor agents: their biological activities and methods of synthesis. *Pharmacol. Rep.*, 2011, **63**, 305-336.
- 36 M. Koba and T. Baczek. Physicochemical interaction of antitumor acridinone derivatives with DNA in view of QSAR studies. *Med. Chem. Res.* 2011, **20**, 1385-1393.
- 37 Q. C. Nguyen, T. T. Nguyen, R. Yougnia, T. Gaslonde, H. Dufat, S. Michel and F. Tillequin. Acronycine Derivatives: A Promising Series of Anti-Cancer Agents. *Anticancer Agents Med. Chem.*, 2009, **9**, 804-815.
- 38 S. Michel, T. Gaslonde and F. Tillequin. Benzo[*b*]acronycine derivatives: a novel class of antitumor agents. *Eur. J. Med. Chem.*, 2004, **39**, 649-655.
- 39 M. Taki, H. Kuroiwa and M. Sisido. Chemoenzymatic Transfer of Fluorescent Non-natural Amino Acids to the N Terminus of a Protein/Peptide. *ChemBioChem*, 2008, **9**, 719-722.
- 40 R. S. G. R. Seixas, A. M. S. Silva, D. C. G. A Pinto and J. A. S. Cavaleiro. A New Synthesis of Benzo[*b*]acridones. *Synlett*, 2008, 3193-3197.
- 41 S. Ronchi, D. Prosperi, C. Thimon, C. Morin and L. Panza. Synthesis of mono- and bisglucuronylated carboranes. *Tetrahedron: Asymmetry*, 2005, **16**, 39-44.
- 42 A. Cappelli, G. P. Mohr, A. Gallelli, G. Giuliani, M. Anzini, S. Vomero, M. Fresta, P. Porcu, E. Maciocco, A. Concas, G. Biggio and A. Donati. Structure-Activity Relationships in Carboxamide Derivatives Based on the Targeted Delivery of Radionuclides and Boron Atoms by Means of Peripheral Benzodiazepine Receptor Ligands. *J. Med. Chem.*, 2003, **46**, 3568-3571.
- 43 E. Vega-Avila and M. K. Pugsley. An Overview of Colorimetric Assay Methods Used to Assess Survival or Proliferation of Mammalian Cells. *Proc. West Pharmacol. Soc.*, 2011, **54**, 10-14.
- 44 A. Irlles, I. C. Gonçalves and M. C. Lopes, A. C. Fernandes, A. G. Ramalho and J. Pertusa. A biological study on the effects of high and low LET radiations following boron neutron capture reaction at the Portuguese Research Reactor. *Physica Medica*, 2001, **17**, 17-19.
- 45 N. G. Oliveira, M. Castro, A. S. Rodrigues, I. C. Gonçalves, C. Martins, J. M. Toscano Rico and J. Rueff. Effect of poly(ADP-ribosyl)ation inhibitors

- on the genotoxic effects of boron neutron capture reaction. *Mutat Res*, 2005, **583**, 36-48.
- 46 A. C. Fernandes, J. P. Santos, J. G. Marques, A. Kling, A. R. Ramos and N. P. Barradas. Validation of the Monte Carlo model supporting core conversion of the Portuguese Research Reactor (RPI) for neutron fluence rate determinations. *Annals of Nuclear Energy*, 2010, **37**, 1139-1145.
- 47 C. Fernandes, I. C. Gonçalves, J. Santos, J. Cardoso, L. Santos, A. F. Carvalho, J. G. Marques, A. Kling, A. J. G. Ramalho and M. Osvay. Dosimetry at the Portuguese Research Reactor using thermoluminescent measurements and Monte Carlo simulations. *Radiation Protection Dosimetry*, 2006, **120**, 349-353.
- 48 A. Wittig, R. L. Moss and W. A. Sauerwein. Glioblastoma, brain metastases and soft tissue sarcoma of extremities: Candidate tumors for BNCT. *Appl. Radiat. Isot.*, 2013, <http://dx.doi.org/10.1016/j.apradiso.2013.11.038i>

